A Framework for Goal Inference Disambiguation for Assistive Robotics

Deepak E. Gopinath and Brenna D. Argall

***Abstract*—Assistive shared-control robots have the potential to transform the lives of millions of people afflicted with severe motor impairments. The usefulness of shared-control robots typically relies on the underlying autonomy's ability to infer the user's needs and intentions *unambiguously* and is often a limiting factor for providing appropriate kinds of assistance confidently and accurately. The contributions of this paper are three-fold: first, we propose a *goal disambiguation* algorithm that enhances the intent inference and assistive capabilities of a shared-control assistive robotic arm. Second, we introduce an *intent inference* algorithm inspired by *dynamic field theory* that works in tandem with the disambiguation scheme. Third, we present a pilot human study with eight subjects to evaluate the efficacy of the disambiguation algorithm. Our results suggest that (a) the disambiguation system is of greater utility for more limited control interfaces and more complex tasks and (b) subjects demonstrated a wide range of disambiguation request behavior with a greater concentration in the earlier parts of the trials.**

***Index Terms*—Assistive Robotics, Shared Autonomy, Intent Inference, Intent Disambiguation**

I. Introduction

ASSISTIVE and rehabilitation machines—such as robotic arms and smart wheelchairs—have the potential to transform the lives of millions of people with severe motor impairments [1]. With rapid technological advancements in the domain of robotics these machines have become more capable and complex and with this complexity the control of these machines has become a greater challenge.

The standard usage of these assistive machines relies on manual teleoperation typically enacted through a control interface such as a joystick. However, greater the motor impairment of the user, the more limited are the interfaces available for them to use. These interfaces (for example, sip-and-puffs and switch-based head arrays) are low-dimensional, discrete interfaces that can only operate in subsets (referred to as *control modes*) of the entire control space. The dimensionality mismatch between the interface and the robot's controllable degrees-of-freedom (DoF) necessitates the user to switch between control modes during teleoperation and has been shown to add to the cognitive and physical burden and affects task performance negatively [2].

As these machines transition into the real world, the introduction of *autonomy* to these assistive machines will likely help to alleviate some of the above-mentioned issues. More specifically, with *shared* autonomy the task responsibility is shared between the user and the underlying autonomy. However, for autonomy to be effective in a shared setting, it needs to have a good idea of the user's needs and intentions. That is, *intent inference* is critical to ensure appropriate assistance.

A straightforward approach to enhance the autonomy's intent inference capabilities is to augment the human-robot system with high-fidelity sensors. However, in the assistive domain, user satisfaction and comfort is of paramount importance and therefore, more sensors can become cumbersome (e.g., if the sensors have to be worn by the user) and expensive very quickly. Therefore, for reasons of user adoption and cost, we intentionally design our assistance add-ons to be as invisible and close to the manual system as possible. As a result, in this work we consider use-case scenarios in which autonomy's inference of user intent is exclusively informed by the human's control commands issued via the control interface (which we assume is completely observable to the autonomy). However, intent inference becomes particularly challenging when the user input is low-dimensional and sparse and the need for intent (goal) *disambiguation* arises in which there are multiple potential goals and the autonomy has to reason about all possibilities before issuing appropriate assistance commands.

Our key insight in this work, is that certain user control commands are *more intent expressive* than others and therefore *may* help the autonomy in improving inference accuracy. More specifically, in this work we investigate how the selection of a subset of the operational control dimensions/modes improves the intent inference and disambiguation capabilities of the robot. As our primary contribution we develop a control mode selection algorithm which selects the control mode *for* the user, in which the user-initiated motion will help the autonomy to *maximally disambiguate* human intent by eliciting more *intent expressive* control commands from the human. Furthermore, as the disambiguation power of our algorithm is closely linked to the fidelity of the underlying intent inference mechanism, as our secondary contribution we also propose a novel intent inference scheme based on ideas from *dynamic field theory* in which the time-evolution of the distribution over goals is specified as continuous-time constrained dynamical system.

In Section II we present an overview of relevant research in the areas of shared autonomy in assistive robotics, types of shared autonomy assistance paradigms, intent inference and synergies in human-robot interaction. Section III presents the mathematical formalism developed for intent disambiguation and inference Section V focuses on the implementation details of the shared control system. The study design and experimental

Deepak E. Gopinath is with the Department of Mechanical Engineering, Northwestern University, Evanston, IL and Shirley Ryan AbilityLab, Chicago, IL.

Brenna D. Argall is with Department of Mechanical Engineering, Department of Electrical Engineering and Computer Science, Northwestern University, Evanston, IL., and Department of Physical Medicine and Rehabilitation, Northwestern University, Chicago, IL., Shirley Ryan AbilityLab, Chicago, IL.

Manuscript received October 31, 2018

methods are discussed in Section VI followed by results in Section VII. Discussion and conclusions are presented in Sections VIII and IX.

II. Related Work

This section provides an overview of related research in the domains of shared autonomy in assistive robotics, intent inference in human-robot interaction and information acquisition in robotics.

Shared-autonomy in assistive systems aims to reduce the user's cognitive and physical burden during task execution without having the user relinquish complete control [3], [4], [5], [6]. In order to offset the drop in task performance due to shifting focus (task switching) from the task at hand to switching between different control modes different mode switch assistance paradigms have been proposed. For example, a simple time-optimal mode switching scheme has shown to improve task performance [2], [7].

Shared control systems often require a good estimate of the human's intent—for example, their intended reaching target in a manipulation task or a target goal location in the environment in a navigation task [8]. Intent can be explicitly communicated by the user [9] using various modalities such as laser pointers, click interfaces and in some cases natural language. Intent can also be inferred from the user's control signals and other environmental cues using various algorithms. Within the context of shared autonomy based teleoperation a Bayesian scheme for user intent prediction is used [10], [11], [12] in which the user is modeled within the Markov Decision Process framework and is typically assumed to be noisily optimizing some cost function for their intended goal. In low-dimensional spaces, this cost function can be learned from expert demonstrations using Inverse Reinforcement Learning [13]. However for high-dimensional spaces such as that of robotic manipulation, learning cost functions that generalize well over the entire space requires large number of samples. In such cases, heuristic cost functions such as sum of squared velocities along a trajectory have been found to be useful for goal prediction [14]. On the other hand simple heuristic approaches can also be used to find direct mappings from instantaneous cues and the underlying human intention. Heuristic approaches can incorporate domain-specific knowledge easily and are computationally less expensive. For example, the use of *instantaneous* confidence functions for estimating intended reaching target in robotic manipulation [15], [5]. However, heuristic methods in general are not sophisticated enough to incorporate histories of states and actions, making them less robust to external noise.

From the robot's perspective, the core idea behind our disambiguation system is that of *"Help Me, Help You"*—that is, if the user can help the robot with more information-rich actions, then the robot in turn can provide accurate and appropriate task assistance more accurately and confidently. A framework for *"people helping robots helping people"* in which the robot relies on semantic information and judgments provided by the human to improve its own capabilities has been developed in [16]. More intent-expressive human actions is related to the idea of legibility in robot actions. In human-robot interaction, the legibility and predictability of robot motion *to* the human has been investigated [17] and various techniques to generate legible robot motion have been proposed [18]. Our work relies on the idea of *inverse legibility* [19] in which the assistance scheme is intended to bring out more legible intent-expressive control commands *from* the human.

III. Mathematical Formalism for Intent Disambiguation

This section describes our intent disambiguation algorithm that computes the control mode that can maximally disambiguate between the goals and the intent inference mechanism that works in conjunction with disambiguation algorithm.

A. Notation

Let $\mathcal{G}$ denote the set of all candidate goals with $n_g = |\mathcal{G}|$ and let g^i refer to the i^{th} goal with $i \in [1, 2, \ldots, n_g]$. A *goal* in this context represents the human's underlying intent. Specifically, in assistive robotic manipulation, since the robotic device is primarily used for reaching toward and grasping of discrete objects in the environment, intent inference is the estimation of the probability distribution over all possible discrete goals (objects) in the environment. At any time t, the autonomy maintains a probability distribution over goals denoted by $\boldsymbol{p}(t)$ such that $\boldsymbol{p}(t) = [p^1(t), p^2(t), \ldots, p^{n_g}(t)]^T$ where $p^i(t)$ denotes the probability associated with goal g^i. The probability $p^i(t)$ represent the robot's confidence that goal g^i is the human's intended goal.

Let $\mathcal{K}$ be the set of all controllable dimensions of the robot and k^i represent the i^{th} control dimension where $i \in [1, 2, \ldots, n_k]$ with $n_k = |\mathcal{K}|$. The limitations of the control interfaces necessitate $\mathcal{K}$ to be partitioned into control modes. Let $\mathcal{M}$ denote the set of all control modes with $n_m = |\mathcal{M}|$. Additionally, let m^i refer to the i^{th} control mode where $i \in [1, 2, \ldots, n_m]$. Each control mode m^i is a subset of $\mathcal{K}$ such that $\bigcup_{i=1}^{n_m} m^i$ spans all of the controllable dimensions. A dimension $k \in \mathcal{K}$ can be an element of multiple control modes.

In this work, we assume a kinematic model for the robot and the kinematic state (the robot's end-effector pose) at any time t is denoted as $\boldsymbol{x}_r(t) \in \mathbb{R}^3 \times \mathbb{S}^3$ and consists of a position and orientation component, where $\mathbb{S}^3$ is the space of all unit quaternions. The pose for goal $g \in \mathcal{G}$ is denoted as $\boldsymbol{x}_g \in \mathbb{R}^3 \times \mathbb{S}^3$. The control command issued by the human via the control interface is denoted as $\boldsymbol{u}_h$ and is mapped to the Cartesian velocity of the robot's end-effector. For a 6DoF robotic arm, $\boldsymbol{u}_h \in \mathbb{R}^6$. The autonomous robot control policy that generates a robot control command is denoted as $\boldsymbol{u}_r \in \mathbb{R}^6$. The control command issued to the robot, which is a synthesis of $\boldsymbol{u}_h$ and $\boldsymbol{u}_r$ is denoted as $\boldsymbol{u} \in \mathbb{R}^6$ (described further in Section V). The control command that corresponds to a unit velocity vector along the positive and negative directions of control dimension k is denoted as $\boldsymbol{e}^k$ and $-\boldsymbol{e}^k$ respectively.

B. Disambiguation Metric

The disambiguation metric that we develop in this paper is a *heuristic* measure that characterizes the intent disambiguation

Algorithm 1 Intent Disambiguation

Require: $\boldsymbol{p}(t_a), \boldsymbol{x}_r(t_a), \Delta t, t_a < t_b < t_c, \boldsymbol{\Theta}$
1: **for** $k = 0 \dots n_k$ **do**
2: Initialize $D_k = 0$, $t = t_a$, $\boldsymbol{u}_h = \boldsymbol{e}^k$
3: **while** $t \leq t_c$ **do**
4: $\boldsymbol{p}_k(t + \Delta t) \leftarrow \text{UpdateIntent}(\boldsymbol{p}_k(t), \boldsymbol{u}_h; \boldsymbol{\Theta})$
5: $\boldsymbol{x}_r(t + \Delta t) \leftarrow \text{SimulateKinematics}(\boldsymbol{x}_r(t), \boldsymbol{u}_h)$
6: **if** $t = t_b$ **then**
7: $Compute\ \ \Gamma_k, \Omega_k, \Lambda_k$
8: **end if**
9: **if** $t = t_c$ **then**
10: $Compute\ \ \Upsilon_k$
11: **end if**
12: $t \leftarrow t + \Delta t$
13: **end while**
14: $Compute\ \ D_k$
15: **end for**

capabilities of a control dimension $k \in \mathcal{K}$ and is denoted as $D_k \in \mathbb{R}$. We explicitly define disambiguation metrics for both positive and negative motions along k as D_k^+ and D_k^- respectively. We also define a disambiguation metric $D_m \in \mathbb{R}$ for each control mode $m \in \mathcal{M}$. By virtue of design, the disambiguation metric D_m is a measure of how useful the user control commands would be *for* the robot to perform more accurate intent inference if the user were to operate the robot in control mode m. Both D_k and D_m will be formally defined in Section III-D. The computation of D_k depends on four features (denoted as Γ_k, Ω_k, Λ_k and Υ_k), that capture different aspects of the *shape* of a projection of the probability distribution over intent. These projections and computations are described in detail in Section III-C and Section III-D, and as a pseudocode in Algorithm 1.

C. Forward Projection of $\boldsymbol{p}(t)$

The first step towards the computation of D_k is model-based forward projection of the probability distribution $\boldsymbol{p}(t)$ from the current time t_a to t_b and t_c ($t_a < t_b < t_c$), Algorithm 1, lines 3-13. We consider two future times (t_b and t_c) in order to compute short-term and long-term evolution of the probability distribution. Application of $\boldsymbol{e}^k$ results in probability distributions $\boldsymbol{p}_k^+(t_b)$, $\boldsymbol{p}_k^+(t_c)$ and $-\boldsymbol{e}^k$ results in $\boldsymbol{p}_k^-(t_b)$ and $\boldsymbol{p}_k^-(t_c)$, where the subscript k captures the fact that the projection is the result of the application of a control command only along control dimension k. All parameters which affect the computation of $\boldsymbol{p}(t)$ are denoted as $\boldsymbol{\Theta}$.

D. Features of D_k

We design four features that encode different aspects of the *shape* of the probability distribution as it evolves under user control in a specific control dimension k. For each control dimension k, each of the four features is computed for projections along both positive and negative directions independently. The four features are computed in lines 7 and 10 in Algorithm 1.

1) *Maximum probability:* The maximum of the projected probability distribution $\boldsymbol{p}_k(t_b)$ is a good measure of the robot's *overall certainty* in accurate predicting human intent (The maximum of this discrete probability distribution is the mode of the distribution). We define the distribution maximum as

$$\Gamma_k = \max_{1 \leq i \leq n_g} p_k^i(t_b). \tag{1}$$

A higher value implies that the robot has a greater confidence in its prediction of the human's intended goal.

2) *Difference between largest probabilities:* Disambiguation accuracy benefits from greater differences between the first and second most probable goals. This difference is denoted as

$$\Omega_k = \max(\boldsymbol{p}_k(t_b)) - \max(\boldsymbol{p}_k(t_b) \setminus \max(\boldsymbol{p}_k(t_b))). \tag{2}$$

Ω_k becomes important in situations in which the distribution can have multiple modes and a measure of overall certainty (Γ_k) alone is not sufficient for successful disambiguation.

3) *Pairwise separation of probabilities:* If the difference between the largest probabilities fails to disambiguate, then the separation, Λ_k, in the remaining goal probabilities will further aid in intent disambiguation. The quantity Λ_k is computed as the *sum of the pairwise distances* between the n_g probabilities.

$$\Lambda_k = \sum_{i=1}^{n_g} \sum_{j=i}^{n_g} |p_k^i(t_b) - p_k^j(t_b)| \tag{3}$$

4) *Gradients:* Γ_k, Ω_k and Λ_k are local measures that encode shape characteristics of the short-term temporal projections of the probability distribution over goals. However, the quantity $\boldsymbol{p}_k(t)$ can undergo significant changes upon long-term continuation of motion along control dimension k. The spatial gradient of $\boldsymbol{p}_k(t)$ encodes this propensity for change and is approximated by

$$\frac{\partial \boldsymbol{p}_k(t)}{\partial x_k} \simeq \frac{\boldsymbol{p}_k(t_c) - \boldsymbol{p}_k(t_b)}{x_k(t_c) - x_k(t_b)}$$

where x_k is the component of robot's projected displacement along control dimension k. The greater the difference between individual spatial gradients, the greater will the probabilities deviate from each other, thereby helping in disambiguation. In order to quantify the "spread" of gradients we define Υ_k as

$$\Upsilon_k = \sum_{i=1}^{n_g} \sum_{j=i}^{n_g} \Big| \frac{\partial p_k^i(t)}{\partial x_k} - \frac{\partial p_k^j(t)}{\partial x_k} \Big| \tag{4}$$

where $|\cdot|$ denotes the absolute value.

5) *Putting it all together:* The individual features Γ_k, Ω_k, Λ_k and Υ_k are then combined to compute D_k in such a way that, by design, higher values of D_k imply greater disambiguation capability for the control dimension k. More specifically,

$$D_k = \underbrace{w \cdot (\Gamma_k \cdot \Omega_k \cdot \Lambda_k)}_{\text{short-term}} + \underbrace{(1 - w) \cdot \Upsilon_k}_{\text{long-term}} \tag{5}$$

where w is a task-specific weight that balances the contributions of the short-term and long-term components (in our implementation, w was set at 0.5 empirically). Equation 5 actually is computed twice, once in each of the positive ($\boldsymbol{e}^k$)

and negative directions ($-\boldsymbol{e}^k$) along k, and the results (D_k^+ and D_k^-) are then summed to compute D_k.

The computation of D_k is performed for each control dimension $k \in \mathcal{K}$. The disambiguation metric D_m for control mode m then is calculated as

$$D_m = \sum_{k \in m} D_k$$

and the control mode with highest disambiguation capability m^* is given by

$$m^* = \underset{m}{\operatorname{argmax}}\, D_m$$

while $k^* = \operatorname{argmax}_k D_k$ gives the control dimension with highest disambiguation capability k^*. Disambiguation mode m^* is the mode that the algorithm chooses *for* the human to better estimate their intent.

IV. Intent Inference

The intent inference approach presented in this section is inspired by *dynamic field theory* (DFT) in which the time evolution of the probability distribution $\boldsymbol{p}(t)$ is specified as a dynamical system with constraints. Dynamic neural fields possess some unique characteristics that make them ideal candidates for modeling higher-level cognition. First, a peak in the activation field can be *sustained* even in the absence of external input due to the recurrent interaction terms. Second, information from the past can be *preserved* over much larger time scales quite easily by tuning the time-scale parameter thereby endowing the variables with memory. Third, the activation fields are *robust* to disturbance and noise in the external output [20]. As a result, DFT principles have found widespread application in the area of cognitive robotics [21], specifically in the contexts of efficient human-robot interaction [22], robotic scene representation [23], obstacle avoidance and target reaching behaviors in both humans and robots [24], and for object learning and recognition [25].

A. Dynamic Neural Fields for Intent Inference

We use the framework of dynamic neural fields to specify the time evolution of the probability distribution $\boldsymbol{p}(t)$, in which we treat the individual goal probabilities $p^i(t)$ as constrained dynamical state variables such that $p^i(t) \in [0, 1]$ and $\Sigma_1^{n_g} p^i(t) = 1$. The time evolution of the probability distribution is given by

$$\frac{\partial \boldsymbol{p}(t)}{\partial t} = \frac{1}{\tau}\Bigg[-\mathbb{I}_{n_g \times n_g} \cdot \boldsymbol{p}(t) + \underbrace{\frac{1}{n_g} \cdot \mathbb{1}_{n_g}}_{\text{rest state}} \Bigg] + \underbrace{\boldsymbol{\lambda}_{n_g \times n_g} \cdot \sigma(\boldsymbol{\xi}(\boldsymbol{u}_h; \boldsymbol{\Theta}))}_{\text{excitatory + inhibitory}} \quad (6)$$

where $\boldsymbol{u}_h$ is the human control input and $\boldsymbol{\Theta}$ represents all other task-relevant features, time-scale parameter τ determines the memory capacity, $\mathbb{I}_{n_g \times n_g}$ is the identity matrix, $\mathbb{1}_{n_g}$ is a vector of dimension n_g containing all ones, $\boldsymbol{\lambda}$ is the control matrix that controls the excitatory and inhibitory aspects, $\boldsymbol{\xi}$ is a function that encodes the nonlinearity through which human control commands and task features affect the time evolution, and σ is a biased sigmoidal nonlinearity given by $\sigma(\boldsymbol{\xi}) = \frac{1}{1+e^{-\boldsymbol{\xi}}} - 0.5$.

The design of $\boldsymbol{\xi}$ is informed by what features of the human control input and environment capture the human's underlying intent most effectively. We rely on the *directedness* of the robot motion towards a goal, the *agreement* between the human commands and robot autonomy and the *proximity* to a goal. With $\boldsymbol{\Theta} = \{\boldsymbol{x}_r, \boldsymbol{x}_{g^i}, \boldsymbol{u}_{r,g^i}\}$, one dimension i of $\boldsymbol{\xi}$ is defined as

$$\xi^i(\boldsymbol{u}_h; \boldsymbol{x}_r, \boldsymbol{x}_{g^i}, \boldsymbol{u}_{r,g^i}) = \underbrace{\frac{1+\eta}{2}}_{\text{directedness}} + \underbrace{\boldsymbol{u}_h^{rot} \cdot \boldsymbol{u}_{r,g^i}^{rot}}_{\text{agreement}} + \underbrace{\max\Big(0, 1 - \frac{\big\|\boldsymbol{x}_{g^i} - \boldsymbol{x}_r\big\|}{R}\Big)}_{\text{proximity}}$$

where $\eta = \frac{\boldsymbol{u}_h^{trans} \cdot (\boldsymbol{x}_{g^i} - \boldsymbol{x}_r)^{trans}}{\|\boldsymbol{u}_h^{trans}\| \|(\boldsymbol{x}_{g^i} - \boldsymbol{x}_r)^{trans}\|}$, $\boldsymbol{u}_{r,g^i}$ is the robot autonomy command for reaching goal g^i, $trans$ and rot refer to the translational and rotational components of a command $\boldsymbol{u}$ or position $\boldsymbol{x}$, R is the radius of the sphere beyond which the proximity component is always zero, and $\|\cdot\|$ is the Euclidean norm. The *directedness* component captures the likelihood of a user taking the shortest straight line path towards a goal g whereas the *agreement* serves as an indicator of the how the human cooperates with autonomy. At every time-step the constraints on $p^i(t)$ are enforced thereby ensuring that $\boldsymbol{p}(t)$ is a valid probability distribution. The most confident goal g^* is computed as $g^* = \operatorname{argmax}_i p^i(t)$.

V. Shared Control

In this work, we use a blending-based shared-control paradigm in which the final robot control command is a linear composition of the human control command and an autonomous robot policy. The autonomous control policy generates control command $\boldsymbol{u}_r \leftarrow f_a(\boldsymbol{x}_r)$ where $f_a(\cdot) \in \mathcal{F}_a$, and $\mathcal{F}_a$ is the set of all control behaviors corresponding to different tasks. This set could be derived using a variety of techniques such as *Learning from Demonstrations* [26], [27], motion planners [28], [29] or navigation functions [30], [31]. Specifically, let $\boldsymbol{u}_{r,g}$ be the autonomy command associated with goal g. The final control command $\boldsymbol{u}$ issued to the robot then is given by

$$\boldsymbol{u} = \alpha \cdot \boldsymbol{u}_{r,g^*} + (1 - \alpha) \cdot \boldsymbol{u}_h$$

where g^* is the most confident goal. Similar to $\boldsymbol{u}_h$, the autonomy command $\boldsymbol{u}_{r,g^*} \in \mathbb{R}^6$ is mapped to the 6D Cartesian velocity of the end-effector. The blending factor α is a piecewise linear function of the probability $p(g^*)$ associated with g^* and is given by

$$\alpha = \begin{cases} 0 & p(g^*) \le \rho_1 \\ \frac{\rho_3(p(g^*) - \rho_1)}{\rho_2 - \rho_1} & \text{if} \quad \rho_1 < p(g^*) \le \rho_2 \\ \rho_3 & p(g^*) > \rho_2 \end{cases}$$

with $\rho_i \in [0, 1] \;\forall\; i \in [1, 2, 3]$ and $\rho_2 > \rho_1$. In our implementation, we empirically set $\rho_1 = \frac{1.2}{n_g}, \rho_2 = \frac{1.4}{n_g}$ and $\rho_3 = 0.7$. The autonomy's control command $\boldsymbol{u}_{r,g}$ is generated using a simple potential field which is defined in all parts of the state space [32]. Every goal g is associated with a potential

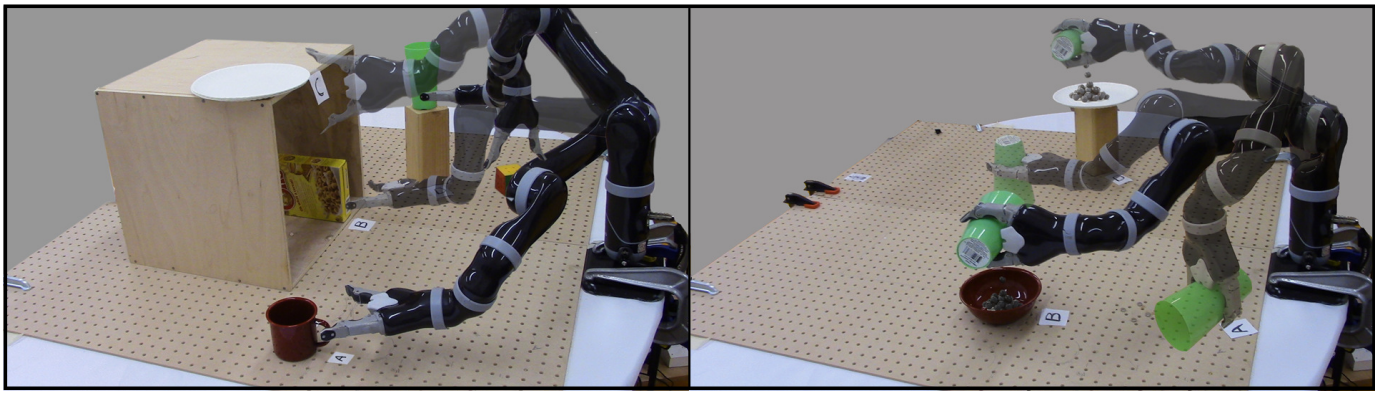

Fig. 1. Study tasks performed by subjects. *Left:* Single-step reaching task. *Right:* Multi-step pouring task.

field γ_g which treats g as an attractor and all the other goals in the scene as repellers. The autonomy command is computed as a summation of the attractor and repeller velocities and operates in the full 6D Cartesian space.

VI. Study Methods

In this section, we describe the study methods used to evaluate the efficacy of the disambiguation system.

Participants: For this study eight subjects were recruited (mean age: 31 ± 11, 3 males and 5 females). All participants gave their informed, signed consent to participate in the experiment, which was approved by Northwestern University's Institutional Review Board.

Hardware: The experiments were performed using the MICO 6-DoF robotic arm (Kinova Robotics, Canada), specifically designed for assistive purposes. The software system was implemented using the Robot Operating System (ROS) and data analysis was performed in MATLAB. The subjects teleoperated the robot using two different control interfaces: a 2-axis joystick and a switch-based head array, controlling the 6D Cartesian velocities of the end-effector (Figure 2). An external button was provided to request the mode switch assistance. For both control interfaces the gripper had a dedicated control mode.

Control Mappings		
Mode	**Head Array**	**Joystick**
1	v_x	v_x, v_y
2	v_y	v_x, v_z
3	v_z	ω_z, ω_y
4	ω_z	ω_x
5	ω_y	—
6	ω_x	—

Fig. 2. A 2-axis joystick (left) and switch-based head array (center) and their operational paradigms (right). v and ω indicate the translational and rotational velocities of the end-effector, respectively. The joystick generates continuous control signals. Under joystick control the full control space is partitioned into four control modes. The switch-based head array consists of three switches embedded in the headrest and generates 1D discrete signals. The back switch is used to cycle between the different control modes, and the switches to the left and right control the motion of the robot's end effector in the positive and negative directions along a selected control dimension. All switches are operated via head movements.

Switching Paradigms: Two kinds of mode switching paradigms were evaluated in the study.

Manual: During task execution the user performed all mode switches.

Disambiguation: The user additionally could request a switch to a *disambiguation* mode at any time during task execution, upon which the algorithm identified and switched the current control mode to the best disambiguating mode m^*. The user was required to request disambiguation at least once during the task execution.

Note that the blending assistance was always active for both paradigms. With blending the amount of assistance was directly proportional to the probability of the most confident goal g^*, and thus to the strength of the intent inference. Therefore, if intent inference improved as a result of goal disambiguation, more assistance would be provided by the robot. All trials started in a randomized initial control mode and robot position.

Study protocol: A within-subjects study was conducted using a fractional factorial design in which the manipulated variables were the tasks, control interfaces and the switching paradigm conditions. Each subject underwent an initial training period that lasted approximately thirty minutes after which the subject performed both tasks using both interfaces under the *Manual* and *Disambiguation* paradigms. The trials were balanced and the control interfaces and the paradigms were randomized and counterbalanced across all subjects to avoid ordering effects. Three trials were collected for the *Manual* paradigm and five trials for the *Disambiguation* paradigm.

Training: The training period consisted of three phases and two different task configurations. The subjects used both interfaces to perform the training tasks.

Phase One: The subjects were asked to perform a simple reaching motion towards a single goal in the scene. This phase was intended for the subjects to get familiarized with the control interface mappings and teleoperation of the robotic arm.

Phase Two: In the second phase of training, subjects experienced how the blending-based autonomy provided assistance during task execution.

Phase Three: For the third phase of the training, multiple objects were introduced in the scene. Subjects were explicitly informed by the experimenter that upon a disambiguation request the robot would select a control mode that would help the robot figure out which goal the subject was going for and thereby enable it to assist the user more effectively.

Subjects were able to explore this request feature during a reaching task, and were instructed to move as much as s/he can in the control mode chosen by the robot and observe the effects of the mode switch request and subsequent change in robot assistance.

Testing: Two different task types were evaluated during testing. Both control interfaces were employed for all tasks.

Single-step: The task is to reach one of five objects on the table, each with a target orientation (Figure 1, Left).

Multi-step: Each trial began with a full cup held by the robot gripper. The task required first that the contents of the cup be poured into one of two containers and then that the cup be placed at one of the two specified locations and with a specific orientation (Figure 1, Right).

Metrics: The objective metrics used for evaluation include the following. *Number of mode switches* refers to the number of times a user switched between various control modes during task execution. *Number of disambiguation requests* refers to the number of times user pressed the disambiguation request button. *Number of button presses* is the sum of *Number of mode switches* and *Number of disambiguation requests*, and is also an indirect measure of user effort. We also characterize the temporal distribution of disambiguation requests using a skewness measure.

VII. Results

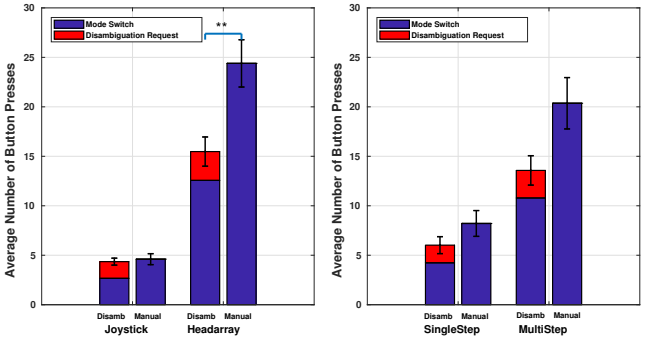

Fig. 3. Comparison of average number of button presses between *Disambiguation* and *Manual* Paradigms. *Left:* Grouped by control interfaces. *Right:* Grouped by tasks.

Here we report the results of our subject study. Statistical significance was determined by the Wilcoxon Rank-Sum test in where (***) indicates $p < 0.001$, (**) $p < 0.01$ and (*) $p < 0.05$.

Impact of Disambiguation on Task Performance: A statistically significant decrease in the number of button presses was observed between the *Manual* and *Disambiguation* paradigms when using the headarray (Figure 3, Left). Due to the low-dimensionality of headarray and cyclical nature of mode switching, the number of button presses required for task completion is inherently high. That the disambiguation paradigm was helpful in reducing the number of button presses likely is due to higher robot assistance in the disambiguating control mode and therefore reduced the need for subsequent user-initiated mode switches. For joystick, statistically significant

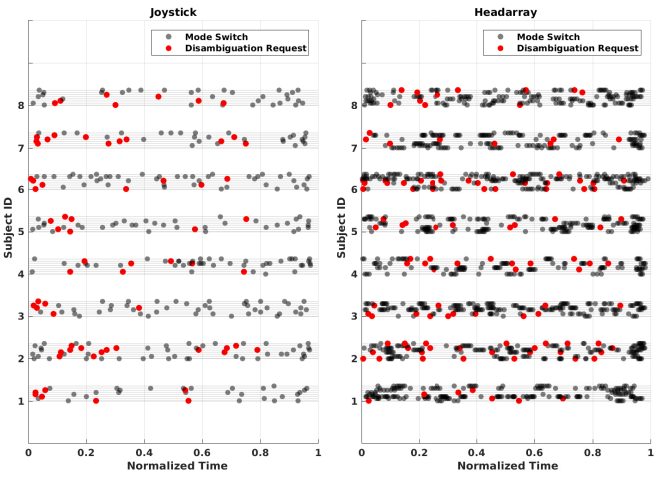

Fig. 4. Temporal pattern of button presses for each interface and the multi-step task on a trial-by-trial basis for all subjects. Eight trials per subject per interface/task combination.

TABLE I
CHARACTERIZATION OF THE TEMPORAL DISTRIBUTION OF DISAMBIGUATION REQUESTS.

	Single Step	Multi Step
Joystick	0.63	0.57
Headarray	0.35	0.22

differences were observed for the number of manual mode switches between the two paradigms ($p < 0.05$, not pictured in Figure 3). However, the gain due to the reduction of user-initiated mode switches was offset by the button presses that were required for disambiguation requests. A general trend (although not statistically significant) of a decrease in the number of button presses was also observed for the more complex multi-step task (Figure 3, Right).

These results suggest that disambiguation is more useful as the control interface becomes more limited and the task becomes more complex. Intuitively, intent prediction becomes harder for the robot when the control interface is low-dimensional and does not reveal a great deal about the user's underlying intent. By having the users operate the robot in the disambiguating mode, the robot is able to elicit more intent-expressive control commands from the human which in turn helps in accurate goal inference and subsequently appropriate robot assistance.

Temporal Distribution of Disambiguation Requests: The temporal distribution of disambiguation requests refers to *when* the subject requested assistance during the course of a trial. We use a measure of *skewness* to characterize how much the temporal distribution deviates from a uniform distribution. Larger positive values of skewness correlate with more concentrated and earlier disambiguation requests. Earlier disambiguation requests is possibly due to the fact that the subjects wanted progress towards the goal to happen right at the start of the trial itself. We observed that a higher number of disambiguation requests correlates with the more limited interface and complex task.

From Figure 4 it is clear that the frequency and density of button presses (disambiguation requests plus mode switches) are much higher for the more limited control interface. The subjects also demonstrated a diverse range of disambiguation request behavior, for example in regards to both when during the execution requests were made and with what frequency (e.g. Subject 8 versus Subject 2, Joystick). The variation between subjects is likely due to different factors such as the user's comfort in operating the robot and understanding the ability of the disambiguating mode to recruit more assistance from the autonomy.

VIII. Discussion

The disambiguation algorithm presented in our work can be utilized in any human-robot system in which there is a need to disambiguate between the different states of a discrete hidden variable can assume (for example, a discrete set of goals in robotic manipulation or a set of landmarks in navigation tasks). Our algorithm also assumes the existence of a discrete set of parameters (for example, control modes for robotic manipulation or natural language-based queries for navigation) that can help the intent inference mechanism to precisely converge to the correct inference. Although the disambiguation algorithm is task-agnostic—because it relies exclusively on the shape features of the probability distribution over the hidden variable—the disambiguation is only as good as the efficacy of the intent inference algorithm that is used for as specific task. In our experience, it becomes important that the choice of cost functions and domain-specific heuristics is appropriate for the task at hand. Furthermore, the efficacy of the disambiguation algorithm degraded when we used only a subset of the four features to inform the disambiguation metric. This only reinforces the need for a combination of different shape features for successful disambiguation. One observation from our subject study was how often participants submitted a disambiguation request, and then chose not to operate in the selected mode—effectively not letting the robot help them. This highlights the need for greater transparency in human-robot interaction so that the human has a clear picture of *how* and *why* the robot chooses to help the user in certain ways. A lack of understanding of how they might help the robot to help them might have resulted in the under-utilization of the disambiguation feature. In order to provide *intent-expressive* control commands to the robot, very likely knowledge of the assistance mechanism is critical. Therefore, the need for extensive and thorough training becomes apparent. The inherent time delays associated with the computation of the disambiguating mode (approximately 2-2.5s) might have been a discouraging factor and a cause for user frustration. The algorithm could be used to pre-compute a large set of most informative modes for different parts of the workspace, goal configurations and priors ahead of time, which then might be used a lookup table during task execution.

In the present system, there is task effort associated with requesting disambiguation assistance which can discourage the users from utilizing the paradigm. Automated mode switching schemes can possibly eliminate the need for button presses for disambiguation requests.

IX. Conclusion

In this paper, we have presented an algorithm for *intent disambiguation assistance* with a shared-control robotic arm using the notion of *inverse legibility*. The goal of our algorithm is to elicit more *intent-expressive* control commands from the user by placing control in those control modes that *maximally disambiguate* between the various goals in the scene. As a secondary contribution, we also present a novel intent inference mechanism inspired by *dynamic field theory* that works in conjunction with the disambiguation system. Pilot user study was conducted with eight subjects to evaluate the efficacy of the disambiguation system. Our results indicate a decrease in task effort in terms of the number of button presses when disambiguation system employed.

In our future work, as informed by our pilot study, we plan to extend the framework into an automated mode switch assistance system. A more extensive user study with motor-impaired subjects will also be conducted in the future to further evaluate the utility of the disambiguation system and explore the disambiguation request patterns of users.

Acknowledgment

This material is based upon work supported by the National Science Foundation under Grant CNS 1544741. Any opinions, findings and conclusions or recommendations expressed in this material are those of the authors and do not necessarily reflect the views of the aforementioned institutions.

References

[1] M. P. LaPlante *et al.*, "Assistive technology devices and home accessibility features: prevalence, payment, need, and trends." *Advance Data from Vital and Health Statistics*, 1992.

[2] L. V. Herlant, R. M. Holladay, and S. S. Srinivasa, "Assistive teleoperation of robot arms via automatic time-optimal mode switching," in *Proceedings of the ACM/IEEE International Conference on Human-Robot Interaction (HRI)*, 2016.

[3] J. Philips, J. d. R. Millán, G. Vanacker, E. Lew, F. Galán, P. W. Ferrez, H. Van Brussel, and M. Nuttin, "Adaptive shared control of a brain-actuated simulated wheelchair," in *Proceedings of the IEEE International Conference on Rehabilitation Robotics (ICORR)*. IEEE, 2007, pp. 408–414.

[4] E. Demeester, A. Hüntemann, D. Vanhooydonck, G. Vanacker, H. Van Brussel, and M. Nuttin, "User-adapted plan recognition and user-adapted shared control: A bayesian approach to semi-autonomous wheelchair driving," *Autonomous Robots*, vol. 24, no. 2, pp. 193–211, 2008.

[5] D. Gopinath, S. Jain, and B. D. Argall, "Human-in-the-loop optimization of shared autonomy in assistive robotics," *IEEE Robotics and Automation Letters*, vol. 2, no. 1, pp. 247–254, 2017.

[6] K. Muelling, A. Venkatraman, J.-S. Valois, J. E. Downey, J. Weiss, S. Javdani, M. Hebert, A. B. Schwartz, J. L. Collinger, and J. A. Bagnell, "Autonomy infused teleoperation with application to brain computer interface controlled manipulation," *Autonomous Robots*, pp. 1–22, 2017.

[7] P. M. Pilarski, M. R. Dawson, T. Degris, J. P. Carey, and R. S. Sutton, "Dynamic switching and real-time machine learning for improved human control of assistive biomedical robots," in *Proceedings of the IEEE RAS & EMBS International Conference on Biomedical Robotics and Biomechatronics (BioRob)* . IEEE, 2012, pp. 296–302.

[8] C. Liu, J. B. Hamrick, J. F. Fisac, A. D. Dragan, J. K. Hedrick, S. S. Sastry, and T. L. Griffiths, "Goal inference improves objective and perceived performance in human-robot collaboration," in *Proceedings of the 2016 International Conference on Autonomous Agents & Multiagent Systems*. International Foundation for Autonomous Agents and Multiagent Systems, 2016, pp. 940–948.

[9] Y. S. Choi, C. D. Anderson, J. D. Glass, and C. C. Kemp, "Laser pointers and a touch screen: intuitive interfaces for autonomous mobile manipulation for the motor impaired," in *Proceedings of the International SIGACCESS Conference on Computers and Accessibility*, 2008.

[10] A. D. Dragan and S. S. Srinivasa, *Formalizing assistive teleoperation*. MIT Press, 2012.

[11] S. Javdani, H. Admoni, S. Pellegrinelli, S. S. Srinivasa, and J. A. Bagnell, "Shared autonomy via hindsight optimization for teleoperation and teaming," *arXiv preprint arXiv:1706.00155*, 2017.

[12] H. Admoni and S. Srinivasa, "Predicting user intent through eye gaze for shared autonomy," in *Proceedings of the AAAI Fall Symposium Series: Shared Autonomy in Research and Practice (AAAI Fall Symposium)*, 2016, pp. 298–303.

[13] B. D. Ziebart, A. L. Maas, J. A. Bagnell, and A. K. Dey, "Maximum entropy inverse reinforcement learning." in *AAAI*, vol. 8. Chicago, IL, USA, 2008, pp. 1433–1438.

[14] A. D. Dragan and S. S. Srinivasa, "A policy-blending formalism for shared control," *The International Journal of Robotics Research*, vol. 32, no. 7, pp. 790–805, 2013.

[15] ——, "Assistive teleoperation for manipulation tasks," in *Proceedings of ACM/IEEE International Conference on Human-Robot Interaction (HRI)*, 2012.

[16] A. Sorokin, D. Berenson, S. S. Srinivasa, and M. Hebert, "People helping robots helping people: Crowdsourcing for grasping novel objects," in *Proceedings of the IEEE/RSJ International Conference on Intelligent Robots and Systems (IROS)*, 2010.

[17] A. D. Dragan, K. C. Lee, and S. S. Srinivasa, "Legibility and predictability of robot motion," in *Proceedings of the ACM/IEEE International Conference on Human-Robot Interaction (HRI)*, 2013.

[18] R. M. Holladay, A. D. Dragan, and S. S. Srinivasa, "Legible robot pointing," in *The IEEE International Symposium on Robot and Human Interactive Communication (RO-MAN)*, 2014.

[19] D. Gopinath and B. Argall, "Mode switch assistance to maximize human intent disambiguation," in *Robotics: Science and Systems*, 2017.

[20] G. Schöner, "Dynamical systems approaches to cognition," *Cambridge Handbook of Computational Cognitive Modeling*, pp. 101–126, 2008.

[21] W. Erlhagen and E. Bicho, "The dynamic neural field approach to cognitive robotics," *Journal of Neural Engineering*, vol. 3, no. 3, p. R36, 2006.

[22] ——, "A dynamic neural field approach to natural and efficient human-robot collaboration," in *Neural Fields*. Springer, 2014, pp. 341–365.

[23] S. K. Zibner, C. Faubel, I. Iossifidis, and G. Schoner, "Dynamic neural fields as building blocks of a cortex-inspired architecture for robotic scene representation," *IEEE Transactions on Autonomous Mental Development*, vol. 3, no. 1, pp. 74–91, 2011.

[24] G. Schöner, M. Dose, and C. Engels, "Dynamics of behavior: Theory and applications for autonomous robot architectures," *Robotics and Autonomous Systems*, vol. 16, no. 2-4, pp. 213–245, 1995.

[25] C. Faubel and G. Schöner, "Learning to recognize objects on the fly: a neurally based dynamic field approach," *Neural Networks*, vol. 21, no. 4, pp. 562–576, 2008.

[26] B. D. Argall, S. Chernova, M. Veloso, and B. Browning, "A survey of robot learning from demonstration," *Robotics and Autonomous Systems*, vol. 57, no. 5, pp. 469–483, 2009.

[27] S. Schaal, "Learning from demonstration," in *Advances in Neural Information Processing Systems*, 1997, pp. 1040–1046.

[28] D. Hsu, R. Kindel, J.-C. Latombe, and S. Rock, "Randomized kinodynamic motion planning with moving obstacles," *The International Journal of Robotics Research*, vol. 21, no. 3, pp. 233–255, 2002.

[29] N. Ratliff, M. Zucker, J. A. Bagnell, and S. Srinivasa, "Chomp: Gradient optimization techniques for efficient motion planning," in *Proceedings of the IEEE International Conference on Robotics and Automation (ICRA)*. IEEE, 2009, pp. 489–494.

[30] E. Rimon and D. E. Koditschek, "Exact robot navigation using artificial potential functions," *IEEE Transactions on Robotics and Automation*, vol. 8, no. 5, pp. 501–518, 1992.

[31] H. G. Tanner, S. G. Loizou, and K. J. Kyriakopoulos, "Nonholonomic navigation and control of cooperating mobile manipulators," *IEEE Transactions on Robotics and Automation*, vol. 19, no. 1, pp. 53–64, 2003.

[32] O. Khatib, "Real-time obstacle avoidance for manipulators and mobile robots," *The International Journal of Robotics Research*, vol. 5, no. 1, pp. 90–98, 1986.